Limnol. Oceanogr., 54(1), 2009, 355–367

The influence of in-stream structures on summer water temperatures via induced hyporheic exchange

Erich T. Hester[1,2]
Curriculum in Ecology, University of North Carolina at Chapel Hill, Chapel Hill, North Carolina 27599

Martin W. Doyle
Department of Geography, University of North Carolina at Chapel Hill, Chapel Hill, North Carolina 27599

Geoffrey C. Poole[3]
Eco-Metrics, Inc., Tucker, Georgia 30084; Odum School of Ecology, University of Georgia, Athens, Georgia 30602

Abstract

Temperature is an important controlling factor for ecological functions. In-stream geomorphic structures affect stream thermal regimes by facilitating hyporheic exchange of water and heat between stream channels and underlying sediments. We varied the height of an experimental weir (representing debris dams, log dams, and boulder weirs) in a small stream during the summer and monitored the hydraulic and thermal response of surface and subsurface water using a three-dimensional sensor array. The presence of the structure altered stream temperature patterns, increasing thermal heterogeneity in surface water and shallow sediments by up to ~1.0°C. We estimated heat conduction and weir-induced hyporheic heat advection across the streambed, and evaluated their response to key parameters. Conduction and advection were of similar magnitude and oscillated over the stream's diel temperature cycle. Weir-induced hyporheic heat advection caused slight cooling of the surface stream (up to ~0.01°C), and increased with weir height, but was considerably less important to the overall heat budget of the stream than was atmospheric heat exchange. Streambed hydraulic conductivity appears to be the overriding factor determining the magnitude of weir-induced hyporheic influence on surface water temperatures. We conclude that weir-type structures will induce ecologically significant surface and subsurface thermal heterogeneity in many stream settings, but that weir-induced hyporheic heat advection will have ecologically significant thermal effects on surface water only in coarse streambeds. Because these structures are common in natural streams and stream restoration projects, such thermal effects may be important on a landscape level.

Temperature is the single most important condition affecting rates of both organism- and ecosystem-level functions (Brown et al. 2004; Begon et al. 2006). Understanding the thermal dynamics of streams is therefore important to understanding ecological stream function. In addition, organisms are adapted to the thermal regimes typically experienced in their native ranges (Hill et al. 2004; Lomolino et al. 2006), and are therefore sensitive to thermal shifts (Walther et al. 2002). Human effects on stream temperature may therefore stress organisms and affect ecosystem function. Consequently, understanding the potential thermal effects of geomorphic features that are common in natural streams and stream restoration projects will be useful for understanding heat dynamics in streams and assessing the ecological effect of stream restoration projects in the context of anthropogenic thermal change.

The hyporheic zone is the area of mixing of surface and groundwater beneath and adjacent to stream channels (Jones and Mulholland 2000). Exchange of water between stream channels and hyporheic zones (hyporheic exchange) facilitates ecologically and biogeochemically important exchanges of heat (Brunke and Gonser 1997; Loheide and Gorelick 2006). In-stream geomorphic structures such as steps, log dams, riffles, and gravel bars are common in natural streams and stream restoration projects, and are known to enhance hyporheic exchange (Kasahara and Wondzell 2003) by creating a hydraulic drop in the channel, which induces curvilinear hyporheic flows paths with downward hyporheic flow upstream of the structure and upward hyporheic flow downstream of the structure (Vaux 1962; Thibodeaux and Boyle 1987; Gooseff et al. 2006). More specifically, this type of hyporheic response has been established for weir-type structures (e.g., debris dams, log dams, and boulder weirs) by modeling (Hester and Doyle 2008) and analogy to underflow patterns for dams (Freeze and Cherry 1979).

Previous studies have characterized the distribution of temperatures in streambed sediments (Ringler and Hall

[1] Corresponding author (ehester@vt.edu).
[2] Present address: Department of Civil and Environmental Engineering, Virginia Tech, Blacksburg, Virginia 24601.
[3] Present address: Department of Land Resources and Environmental Sciences, Montana State University, Bozeman, Montana 59717.

Acknowledgments

Myles Killar, Meredith Harvill, Jason Johnson, and Frank M. Smith provided valuable field assistance and data analysis. Two anonymous reviewers provided valuable comments that significantly improved the manuscript. This work was supported by a United States Environmental Protection Agency (EPA) Science to Achieve Results (STAR) graduate fellowship to E.T.H. and by a National Science Foundation (NSF) grant to M.W.D. (CAREER-BCS-0441504). The EPA has not officially endorsed this publication and the views expressed herein may not reflect the views of the EPA.

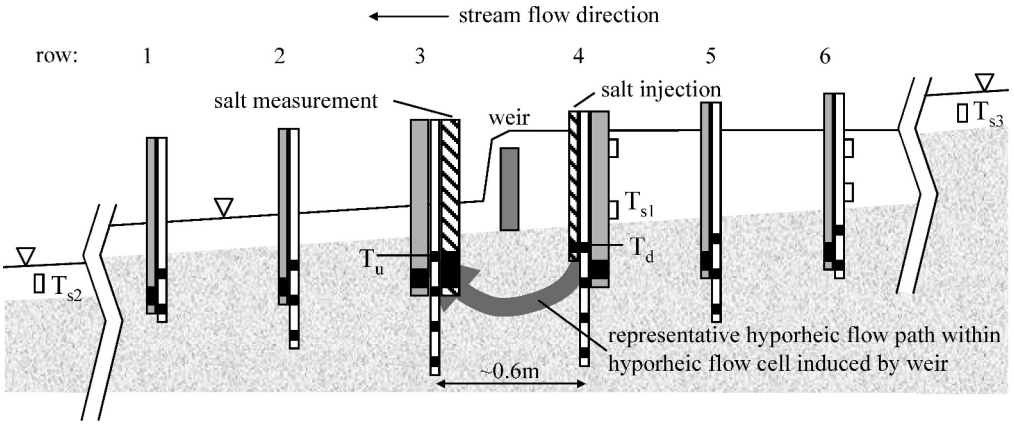

Fig. 1. Schematic showing longitudinal arrangement of piezometers. Piezometers shaded gray were used for measuring hydraulic head along centerline of channel. Piezometers shown in white were used for measuring temperature in two longitudinal columns, one each approximately 0.23 m to the left and right of the central column of hydraulic piezometers (only one column of temperature piezometers shown). Areas shaded black indicate piezometer screen locations. Temperature sensors (iButtons) were located at each well screen shown, with baffles inserted between sensors to isolate the water in each piezometer in vertical intervals. Piezometers shaded with diagonal stripes were used for injection of salt solution into the hyporheic zone upstream of the weir and measurement of the salt breakthrough curve using a conductivity logger downstream of the weir. Temperature sensor locations in the surface stream are indicated by open rectangles. Water surface is indicated by inverted triangles.

1975; Crisp 1990), and related temperature patterns to sediment pore-water movement (Hansen 1975; Silliman and Booth 1993) and heat flux (Hondzo and Stefan 1994; Moore et al. 2005). Such patterns have also been used to distinguish areas of upward and downward hyporheic flow (Lapham 1989; Stonestrom and Constantz 2003). The connection between geomorphic form and hyporheic exchange of water and heat in streams and rivers has been well documented (Fernald et al. 2006; Arrigoni et al. 2008; Poole et al. 2008). For example, distinct water exchange patterns and associated hyporheic temperature patterns have been documented for specific types of in-stream structures, such as riffles (White et al. 1987; Evans and Petts 1997), dunes (Cardenas and Wilson 2007), and steps (Moore et al. 2005). Nevertheless, we are unaware of prior studies that have experimentally manipulated in-stream structures to determine resulting effects on hyporheic temperature, heat exchange across the streambed (streambed heat flux), and surface stream temperature.

Net heat flux across the streambed induced by hyporheic water exchange (hyporheic heat advection) can moderate benthic and surface stream temperatures over diel and annual cycles (Lapham 1989; Loheide and Gorelick 2006). Relative to diel or annual temperature cycles in the surface stream, temperature cycles in upwelling hyporheic water may have a different daily average temperature (i.e., may be cooler or warmer), a reduced diel temperature range (i.e., may be buffered) or a delayed phase (i.e., may be lagged) (Arrigoni et al. 2008). Because of the ecological importance of temperature, understanding the relationships between geomorphology and temperature will then be useful for understanding the thermal dynamics of streams and the effects of stream restoration projects in the context of human effects on stream temperatures. The goals of our study were therefore to determine the effect of weir-type in-stream geomorphic structure presence and size on (1) hyporheic temperature patterns, (2) structure-induced hyporheic heat advection, and (3) surface stream temperature.

Methods

Field experiments—We performed field experiments during the summers of 2006 and 2007 in a first-order headwater reach of Craig Creek in the Jefferson National Forest near Blacksburg, Virginia. The stream surface is 1–2 m wide with baseflow discharge of 0.5–5.0 L s^{-1} and hydrologically neutral to gaining conditions. The reach is a fairly straight 10-m-long riffle located between pools at the adjacent upstream and downstream meander bends. It has a gravel and cobble surface substrate, with increasing proportions of sand at depth.

We constructed a single, channel-spanning, variable-height weir perpendicular to the channel (Fig. 1). The weir was intended to represent both naturally formed structures (e.g., debris dams created when trees or large woody debris fall across the channel) and manmade structures (e.g., log or boulder weirs in stream restoration projects). The weir was not keyed into the substrate and thus did not inhibit induced hyporheic flow paths beneath the structure (Hester and Doyle 2008). Subsurface water levels were measured with automatic stage recorders (Onset U20-001-01 hobos) and manual well sounder readings (using Solinst Model 101M) in a series of six piezometers distributed longitudinally along the centerline of the channel upstream and downstream of the weir (shaded piezometers in Fig. 1) and screened at approximately 0.23 m below the streambed surface. Water levels in the surface stream were measured along the right side of the channel with automatic stage recorders (Onset U20-001-01 hobo and Intech WT-HR 1000) installed in perforated pipes at rows 3 and 4, and with manual stage gauges located at rows 1, 2, 4, and 6 (Fig. 1). Surface stream stages were also measured along the centerline of the channel using manual well sounder

Table 1. Values and sources for input parameters used in hydraulic and thermal calculations.

Parameter	Symbol	Units	Value	Source
Area of streambed where weir-induced hyporheic flow enters subsurface upstream of weir	A_d	m^2	0.99 (2006) 1.07 (2007)*	Measured
Area of streambed where weir-induced hyporheic flow discharges to surface stream downstream of weir	A_u	m^2	6.5	Estimated using Eq. 4, averaged across both years
Area of streambed used for streambed heat conduction heat flux calculations	A_c	m^2	7.5	Sum of A_d and A_u averaged across both years
Specific heat of sand and water, bulk	C_{bs}	J kg^{-1} $°C^{-1}$	1372	Jobson (1977)
Specific heat of water	C_w	J kg^{-1} $°C^{-1}$	4187	Lindeburg (2001)
Hydraulic head difference between surface stream and subsurface water	Δh	m	Varies hourly, multiple locations	Measured
Estimated hydraulic conductivity of sediments in area used for Eq. 3	K	m s^{-1}	1.39×10^{-5} (2006, $n=2$) 4.54×10^{-5} (2007, $n=3$)	Geometric mean of hydraulic conductivities measured by falling-head tests in streambed piezometers
Downward hyporheic flow rate	Q_d	m^3 s^{-1}	Varies hourly	Estimated using Eq. 2
Surface stream discharge	Q_s	m^3 s^{-1}	Varies hourly	Measured
Darcy velocity	q	m s^{-1}	Varies hourly	$=Ki_d$
Temperature of subsurface water at conduction depth	T_c	°C	Varies hourly, multiple locations	Measured, used deepest iButtons available at each location
Temperature of surface stream water immediately above the area of downward hyporheic flow upstream of the weir (T_{s1}, Fig. 1)	T_{s1}	°C	Varies hourly	Measured
Temperature of surface stream water downstream of the weir (T_{s2}, Fig. 1)	T_{s2}	°C	Varies hourly	Measured
Temperature of surface stream water upstream of the weir backwater (T_{s3}, Fig. 1)	T_{s3}	°C	Varies hourly	Measured
Temperature of upward hyporheic flow downstream of weir (T_u, Fig. 1)	T_u	°C	Varies hourly, multiple locations	Measured
Depth of piezometer screen used for estimating vertical hydraulic gradient	Δz	m	0.23 (2006) 0.235 (2007)	Measured
Vertical distance between conduction depth and sediment surface	Δz_c	m	Multiple locations and years; 0.435–0.575 m	Measured
Thermal diffusivity of sand and water, bulk	λ_{bs}	m^2 s^{-1}	7.7×10^{-7}	Jobson (1977)
Density of water	ρ_w	kg m^{-3}	1000	Lindeburg (2001)
Bulk density of sand and water, average density, mixed grain size	ρ_{bs}	kg m^{-3}	2075	Lindeburg (2001)
Thermal oscillation period	τ	s	86,400	

* Channel was slightly wider and sediments slightly more hydraulically conductive in 2007 than in 2006 because of effects of intervening winter storms.

readings with the Solinst 101M on the outside of the hydraulic piezometers in rows 1–6 (shaded gray in Fig. 1). Salt slug tracer injections were conducted to measure residence time of hyporheic water in the subsurface (Hester and Doyle 2008) (piezometers with diagonal stripes in Fig. 1) and surface stream discharge (Moore 2005).

Temperatures were measured with a three-dimensional array of Thermochron iButton temperature sensor–loggers (models DS1921-Z and DS1921-H, Dallas Semiconductor) placed in two columns of piezometers in the streambed (white piezometers in Fig. 1) and mounted in the surface stream both in the pool formed behind the weir and further upstream and downstream (Fig. 1). Temperature data were calibrated using correction factors specific to each individual sensor. Correction factors were determined by noting the difference in temperature readings between each iButton and highly accurate American Society for Testing and Materials mercury thermometers when placed in each of several constant-temperature water baths that spanned the range of temperatures observed in the field experiments. Calibration improved the accuracy of the iButton data from ±1.0°C as reported by the manufacturer (http://www.ibutton.com) to approximately ±0.1°C (fig. 3 of Johnson et al. 2005).

Calculations—We used hydraulic and temperature data to estimate a variety of hydraulic and thermal quantities. Values and sources for input parameters used in the calculations are listed in Table 1.

Vertical hydraulic gradient: We calculated the vertical hydraulic gradient between the surface stream and subsurface water (i, defined as negative when downward into the streambed) (m m^{-1}) for a variety of locations as

$$i \equiv \frac{\Delta h}{\Delta z} \tag{1}$$

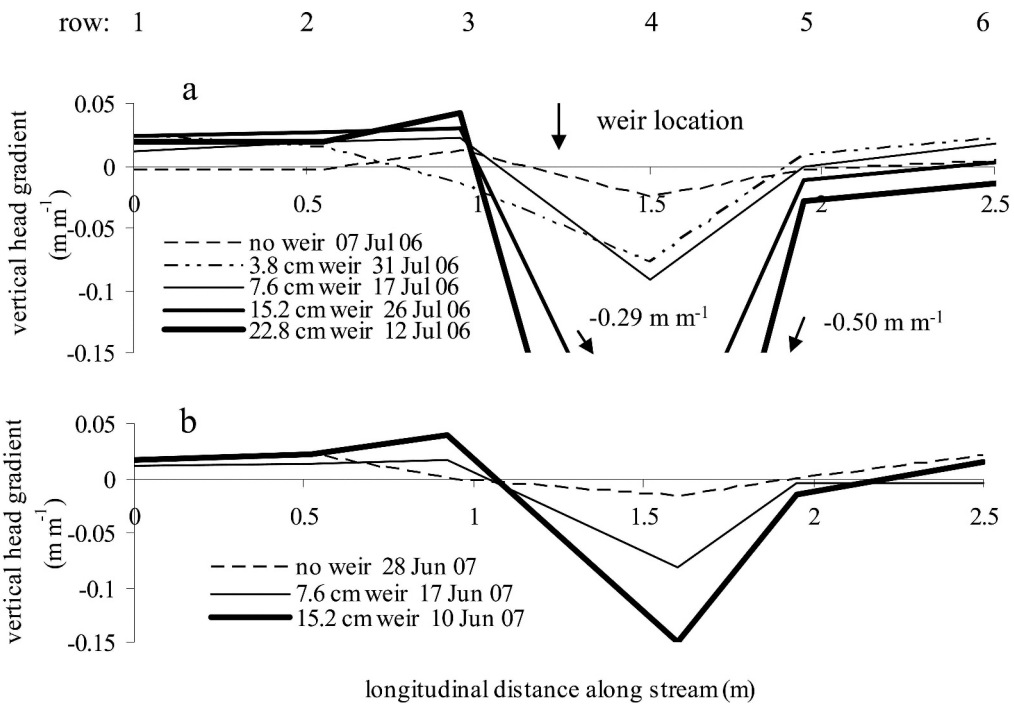

Fig. 2. Representative longitudinal profiles of channel center vertical hydraulic gradients between surface stream and subsurface water for (a) 2006 and (b) 2007. Row numbers indicate piezometers rows as in Fig. 1.

where Δh is the hydraulic head difference between the piezometer and the surface stream adjacent to the piezometer (m) and Δz is the difference in elevation between the piezometer screen and the streambed surface adjacent to the piezometer (m) (Table 1).

Advective heat flux: We estimated downward flow of water across the streambed from the surface stream into the hyporheic zone upstream of the weir ($m^3\ s^{-1}$) (downward hyporheic flow rate, Q_d) using Darcy's Law:

$$Q_d = Ki_dA_d \quad (2)$$

where K is the hydraulic conductivity of the sediments ($m\ s^{-1}$), i_d is the hydraulic gradient upstream of the weir ($m\ m^{-1}$), and A_d is the area of downward hyporheic flow across the streambed (m^2) (Table 1). Equation 2 utilized hourly hydraulic data from the first piezometer upstream of the weir (row 4 in Fig. 1). These hydraulic data were applied to the area A_d, which extends from the weir upstream to midway between piezometer rows 4 and 5 and across the full width of the channel. We chose the area closest to the weir because hydraulic gradients were strongest there (*see* Results; Fig. 2) indicating that most of the downward hyporheic flow induced by the weir occurred near the weir, regardless of weir height. Although not shown in Fig. 2, head gradients would be even higher at the upstream face of the weir than at piezometer row 4 because of a gradient discontinuity at the weir (Hester and Doyle 2008), such that piezometer row 4 is reasonably representative of area A_d.

We estimated net heat flux across the streambed caused by weir-induced flow of water through the hyporheic flow cell (hyporheic heat advection, J_a) ($J\ s^{-1}$) on an hourly basis by (Moore et al. 2005)

$$J_a = \rho_w C_w Q_d (T_u - T_{s1}) = \rho_w C_w K i_d A_d (T_u - T_{s1}) \quad (3)$$

where ρ_w is the density of water ($kg\ m^{-3}$), C_w is the specific heat of water ($J\ kg^{-1}\ °C^{-1}$), T_u is the temperature of upward hyporheic flow discharging to the surface stream downstream of the weir (°C), and T_{s1} is the temperature of surface stream water immediately above the area of downward hyporheic flow upstream of the weir (°C) (Table 1; Fig. 1). Equation 3 assumes that water induced into the hyporheic zone upstream of the weir in the area specified by A_d flows downstream beneath the weir and then returns to the surface stream by upward hyporheic flow downstream of the weir in an area specified by A_u (m^2), forming a weir-induced hyporheic flow cell (Hester and Doyle 2008). This assumption is an approximation, but is reasonable given that the net hydrologic balance of our study reach was neutral to slightly gaining, and the exploratory nature of our analysis (Moore et al. 2005). We were unable to measure A_u directly, but because the same hyporheic flow (Q_d) passes through both A_d and A_u, and because we assume sediment hydraulic conductivity (K) remains constant (Table 1), we estimate A_u as

$$A_u = A_d \frac{-i_d}{i_u} \quad (4)$$

where i_u is the hydraulic gradient at the end of the hyporheic flow cell (i.e., downstream of the weir) ($m\ m^{-1}$). We estimated T_u (Table 1) by averaging temperatures from the two iButton piezometer locations closest to the weir (row 3, Fig. 1) because the greatest flow occurs in this area (*see* Results; Fig. 2).

Conductive heat flux: We estimated net heat flux between the surface stream and subsurface water caused by vertical conduction (streambed heat conduction, J_c) on an hourly basis (J s^{-1}) by (Moore et al. 2005)

$$J_c = \rho_{bs} C_{bs} A_c \lambda_{bs} \frac{T_c - T_{s1,2}}{\Delta z_c} \quad (5)$$

where ρ_{bs} is the bulk density of saturated sand (kg m^{-3}), C_{bs} is the specific heat of saturated sand (J kg^{-1} $°C^{-1}$), A_c is the area of the streambed of interest (m^2), λ_{bs} is the thermal diffusivity of saturated sand (m^2 s^{-1}), T_c is the temperature of subsurface water at depth (°C), $T_{s1,2}$ represents the temperature of surface stream water above the sediment (°C), and Δz_c is the depth of the subsurface temperature measurement T_c (m) (Table 1; Fig. 1). Equation 5 utilized hourly temperature data to calculate streambed heat conduction. A_c was set equal to the sum of A_d and A_u, averaged across all weir heights and both years (Table 1) to allow estimated streambed heat conduction to be compared with estimated weir-induced hyporheic heat advection. We divided A_c into four sections (corresponding to piezometers in rows 3 and 4, left and right), calculated conduction for each section, and summed the four sections, providing the net flux rate for the area A_c. The relative dominance of advective and conductive processes can be quantified as (Cardenas and Wilson 2007)

$$Pe = q\sqrt{\frac{\tau}{\pi \lambda_{bs}}} \quad (6)$$

where Pe is the Peclet number for heat flow at the location where surface water enters the hyporheic flow cell upstream of the weir (dimensionless), q is the average Darcy velocity (m s^{-1}; $=Ki_d$), and τ is the period of thermal oscillation (s) (Table 1).

Response of surface stream temperatures: We estimated the effect of weir-induced hyporheic heat advection calculated by Eq. 3 on surface stream temperatures (ΔT_a) (°C) by (Story et al. 2003):

$$\Delta T_a = \frac{Q_d}{Q_s}(T_u - T_{s3}) = \frac{K i_d A_d}{Q_s}(T_u - T_{s3}) \quad (7)$$

where Q_s is the discharge in the surface stream (m^3 s^{-1}) and T_{s3} is the temperature of surface stream water upstream of the weir backwater area (°C) (Table 1; Fig. 1). Equation 7 estimates the influence of weir-induced hyporheic heat advection in isolation, independent of streambed heat conduction or atmospheric heat fluxes. Equation 7 applies to a length of stream that includes just the hyporheic flow cell induced by the weir (i.e., encompassing A_d and A_u as defined previously), and hence no other water fluxes crossing the streambed. Although J_a does not explicitly appear in Eq. 7, its effect manifests through Q_d and T_u, which are the same for both Eq. 3 and Eq. 7.

Results

Hydraulics—In the presence of the weir, vertical hydraulic gradient (i) along the channel centerline was generally downward upstream of the weir, and upward downstream of the weir (Fig. 2). This pattern was much weaker or nonexistent in the absence of the weir. Among the representative vertical head gradient profiles in Fig. 2, hydraulic gradient just upstream of the weir (i_d, piezometer row 4) tended to increase in magnitude with weir height to -0.50 m m^{-1} for the 22.8-cm-high weir in 2006, and -0.15 m m^{-1} for the 15.2-cm weir in 2007. Conversely, hydraulic gradient just downstream of the weir (i_u, piezometer row 3) reached 0.04 m m^{-1} for the 22.8-cm-high weir in 2006 and the 15.2-cm weir in 2007. By comparison, in the absence of a weir, downward and upward hydraulic gradients never exceeded -0.03 m m^{-1} and 0.02 m m^{-1}, respectively, for both years combined. Because the magnitude of i_d exceeds that of i_u, A_u is larger than A_d (Eq. 4). A_u/A_d varied considerably based on variations in weir height, surface stream discharge, and other factors, but was always 3.0 or greater. Consistent with the vertical hydraulic gradient data, diel temperature oscillations penetrated deeper into subsurface upstream of the weir than downstream of the weir whenever a weir was present, and this pattern abated in the absence of the weir (Fig. 3).

Subsurface water temperatures—Shallow subsurface water warmed up during the afternoon with or without a weir present (Figs. 4a, 5). However, when a weir was present, heating extended further into subsurface upstream of the weir, creating a drop in temperature in the shallow hyporheic zone upstream (T_d; Fig. 1) to downstream (T_u; Fig. 1) across the weir, both during the day (up to approximately 1.5°C; Fig. 4a) and averaged over the diel cycle (up to approximately 0.5°C; Figs. 4c, 5). Furthermore, T_u was generally cooled (lower daily average temperature; Fig. 4c), buffered (smaller daily temperature range; Fig. 4d), and lagged (delayed phase of temperature peaks and/or troughs; Fig. 6) relative to T_{s1} and T_d.

Streambed heat flux—Net heat conduction across the streambed (streambed heat conduction, J_c) and net weir-induced hyporheic heat advection across the streambed (hyporheic heat advection, J_a) exhibited diel cycles in which net heat flux is from the surface stream to the subsurface (i.e., cooling effect on surface water) over much of the day and net heat flux is from the subsurface to the surface stream (i.e., warming effect on surface water) for a short period in early morning (Fig. 7a), mirroring temperature differences between the surface stream and the subsurface (Fig. 7b). Average daily total weir-induced hyporheic heat advection was always negative (i.e., cooling effect on surface water), and increased in magnitude with weir height (Fig. 8a), from approximately -300 kJ d^{-1} for a 3.8-cm weir to -1600 kJ d^{-1} for a 22.8-cm weir (~450% increase) in 2006, and from approximately -300 kJ d^{-1} for a 7.6-cm weir to -1200 kJ d^{-1} for a 15.2-cm weir (~300% increase) in 2007. Average Peclet number similarly increased with weir height from 0.21 for a 3.8-cm weir to 1.20 for a 22.8-cm weir (Fig. 8c; ~470% increase). Using linear regression, the coefficients of determination (R^2) for daily total weir-induced hyporheic heat advection vs. weir

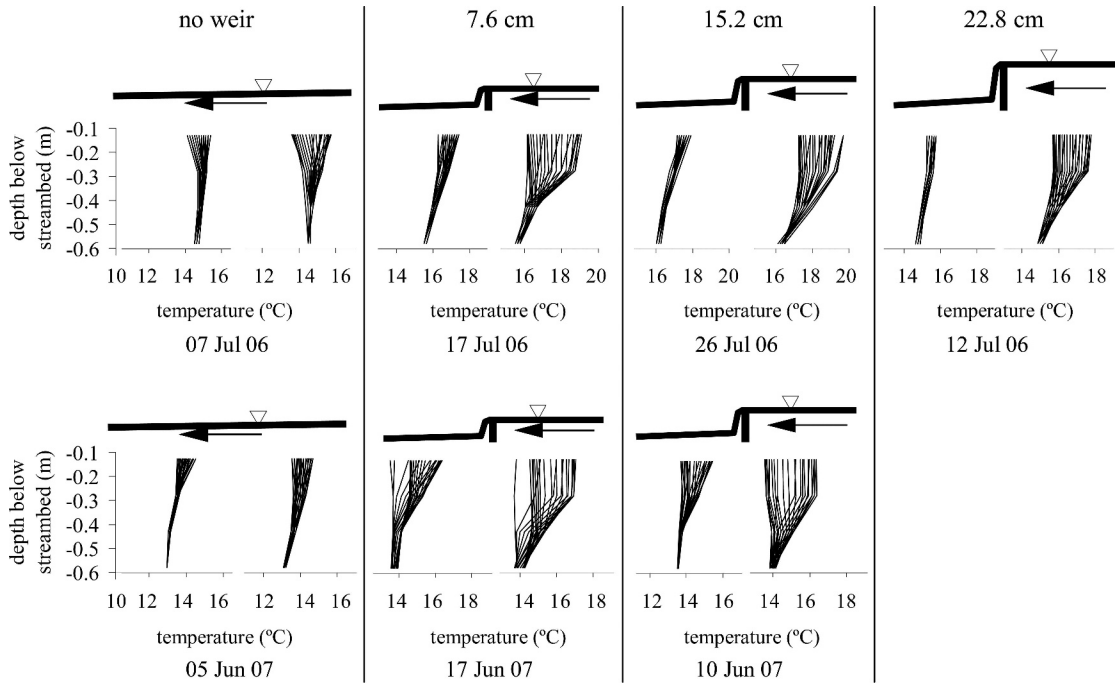

Fig. 3. Profiles of subsurface water temperature vs. depth below streambed for the 24-h periods beginning at 10:00 h on the dates shown. Each profile contains separate lines for each of 24 separate hourly intervals spanning the day specified. Left and right profiles for each weir height and year combination are for downstream (row 3 in Fig. 1) and upstream (row 4 in Fig. 1) of the weir, respectively. Corresponding weir heights are shown across the top. Results from 2006 and 2007 are shown in the first and second row of the figure, respectively. Longitudinal water surface schematics immediately above each plot are for visual orientation and are not to scale (inverted triangles indicate water surface, arrows indicate direction of flow). Plots shown are for left-hand column of temperature piezometers (*see* Fig. 1); results for right-hand column are similar but not shown.

height were 0.59 and 0.68 for the 2006 and 2007 data, respectively, and 0.59 for both years combined. The slopes of all regression lines were significantly different from zero ($p < 0.01$). The magnitude of average daily total streambed heat conduction was always greater than weir-induced hyporheic heat advection (note y-axis scales in Fig. 8) and was similarly a consistent cooling influence on the surface stream, ranging from -3800 kJ d^{-1} to -7500 kJ d^{-1} in 2006, and from -2700 kJ d^{-1} to -4400 kJ d^{-1} in 2007. There was not a consistent conduction response to weir height (Fig. 8b). Using linear regression, R^2 values for daily total streambed heat conduction vs. weir height were 0.46 and 0.26 for 2006 and 2007, respectively, and 0.20 for both years combined. The slopes of the regression lines were different from zero at varying levels of significance ($p < 0.01$ and $p < 0.1$ for the 2006 and 2007 data, respectively, and $p < 0.01$ for both years combined).

Surface stream temperatures—The estimated effect of weir-induced hyporheic heat advection on surface stream temperatures (ΔT_a; Fig. 9) followed the same diel pattern as hyporheic heat advection (Fig. 7) with cooling over much of the day and warming in early morning (up to $\sim$0.01°C in magnitude). The observed temperature changes that occurred as stream water flowed across the weir were estimated as the difference between stream temperatures downstream of the weir and stream temperatures upstream of the weir's backwater (T_{s2} and T_{s3} in Fig. 1), were generally much greater than the estimated effect of weir-induced hyporheic heat advection, and did not appear to follow the same diel cycle (up to $\sim$0.4°C in magnitude; Fig. 9). The daily average effect of weir-induced hyporheic heat advection was cooling from the perspective of the surface stream, and increased in magnitude with weir height from -0.001°C at 7.6 cm to -0.003°C at 15.2 cm for 2007 (Fig. 10a). In comparison, the daily average observed temperature change across the weir ($T_{s2} - T_{s3}$; Fig. 1) ranged from -0.01°C to 0.03°C, but exhibited no discernible trend with weir height (Fig. 10b; $R^2 = 0.04$). In addition, when a weir was present, thermal heterogeneity was observed in surface water upstream of the weir both during the day (up to $\sim$1.0°C; Fig. 4a) and averaged over the diel cycle (up to $\sim$0.5°C; Fig. 4c).

Discussion

Hydraulics—Hydraulic data collected at the site confirmed that backwater created by the weir produced a curved hyporheic flow cell (Fig. 1) that is expected based on the literature (Freeze and Cherry 1979; Hester and Doyle 2008). The roughly vertical component of hyporheic flow at either end of the hyporheic flow cell was confirmed by longitudinal patterns of vertical head gradient along the channel centerline (Fig. 2), which indicated downward hyporheic flow upstream of the weir and upward hyporheic flow downstream of the weir. Further, vertical subsurface water temperature profiles upstream and downstream of the weir (Fig. 3) showed deeper and shallower subsurface

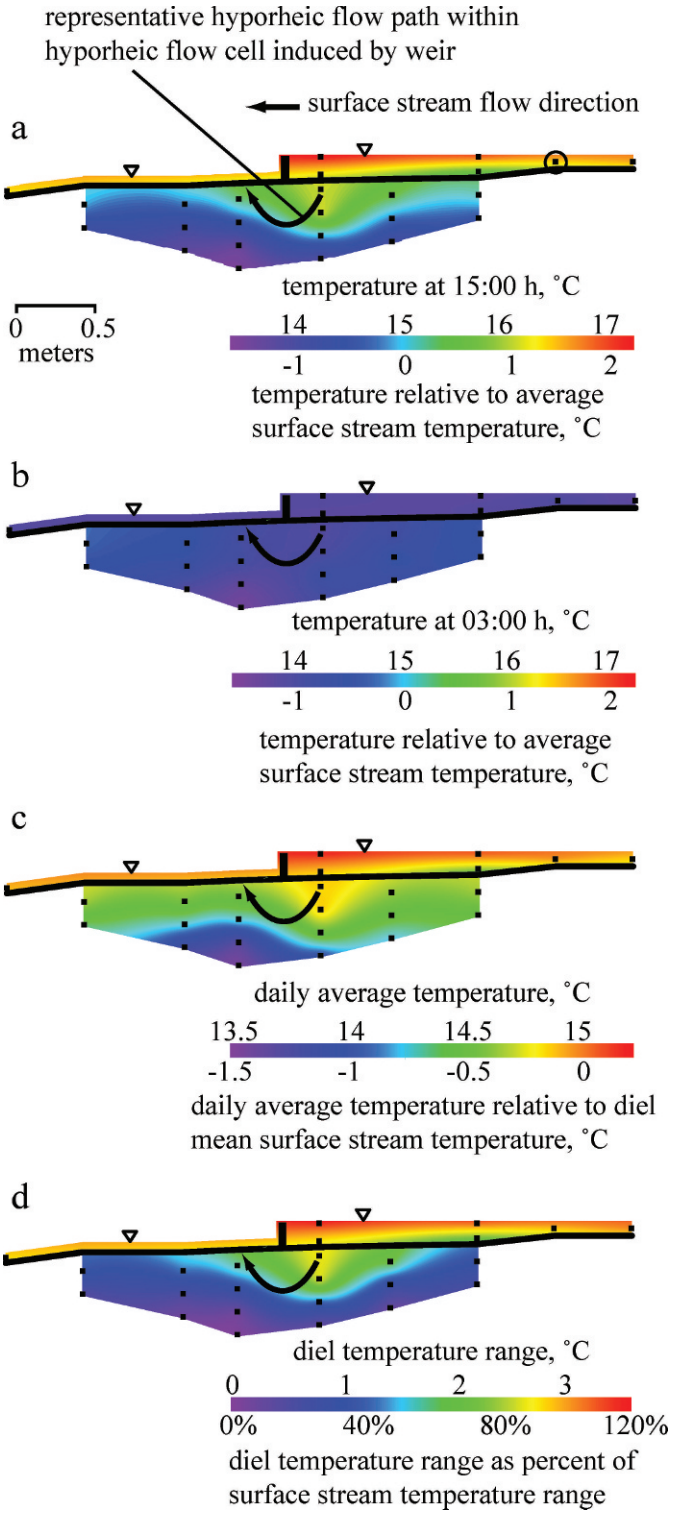

Fig. 4. Example longitudinal vertical slices through subsurface and surface water temperature data for the 15.2-cm weir on representative day (10 June 2007). Shown are (a) temperature at 15:00 h, (b) temperature at 03:00 h the next morning, (c) daily average temperature, and (d) diel temperature range. Relative temperature scales beneath color bars are relative to temperatures (a, b), daily average temperatures (c), or diel temperature ranges (d) for surface stream location marked by open circle in 4a. Filled squares show locations of iButton sensors; inverted triangles indicate water surface. Subsurface iButtons are for left column of iButtons (*see* Methods; Fig. 1) because of its more complete data set. The surface water iButton locations downstream and upstream of the hyporheic zone measurements are not shown to scale (horizontal scale is compressed relative to rest of figure). Plots created using Surfer with kriging interpolation using default settings.

penetration of diel temperature oscillations, respectively, indicating areas of downward and upward hyporheic flow (Lapham 1989). The horizontal component of weir-induced hyporheic flow in the downstream direction beneath the weir was confirmed by tracer tests (Hester and Doyle 2008) in which slugs of concentrated salt solution injected into subsurface water upstream of the weir were consistently detected in subsurface water downstream of the weir (*see* Fig. 1 for injection and monitoring piezometer locations). Hydraulic data (Hester and Doyle 2008) also indicate that downward hydraulic gradient upstream of the weir (i_d, row 4 in Fig. 1) and therefore downward hyporheic flow rate (Q_d, Eq. 2) increases consistently with weir height, which is important for interpreting weir-induced hyporheic heat advection results (below). Upwelling area (A_u) consistently greater than downwelling area (A_d) indicates divergence of hyporheic flow paths from upstream to downstream, as expected for weir-type structures (Hester and Doyle 2008).

Temperatures and streambed heat flux—Surface and subsurface water temperature patterns at our experimental site exhibited a number of important characteristics even in the absence of a weir. First, surface stream water was warmer on average than groundwater beneath, and hyporheic water showed a gradation of temperatures between the two end points (Figs. 3, 4c). Second, diel temperature oscillations were observed in both surface stream and subsurface water, with subsurface oscillations being buffered and lagged relative to the surface stream and with increasing depth (Figs. 3, 4d, 5, 6). This suite of summer stream temperature patterns has been widely reported (Lapham 1989; Stonestrom and Constantz 2003; Arrigoni et al. 2008) and is caused by oscillation in atmospheric heating of the surface stream on annual and diel cycles, which propagates into subsurface water beneath by conduction and sometimes advection of heat across the streambed (Lapham 1989; Silliman and Booth 1993).

Effect of weir presence and height: The addition of the weir to the experimental site increased average temperature in the shallow hyporheic zone upstream of the weir, creating a drop in average temperature in the shallow hyporheic zone upstream to downstream across the weir (Figs. 4c, 5). The presence of the weir probably affected temperatures in the ecologically important (Hynes 1970) benthic zone in a similar fashion, although we did not measure temperatures in the shallowest sediments (<10-cm depth). This hyporheic temperature modification was caused by advection of heat from the warmer (on average) surface stream through the weir-induced hyporheic flow cell. On average, hyporheic water cooled as it flowed

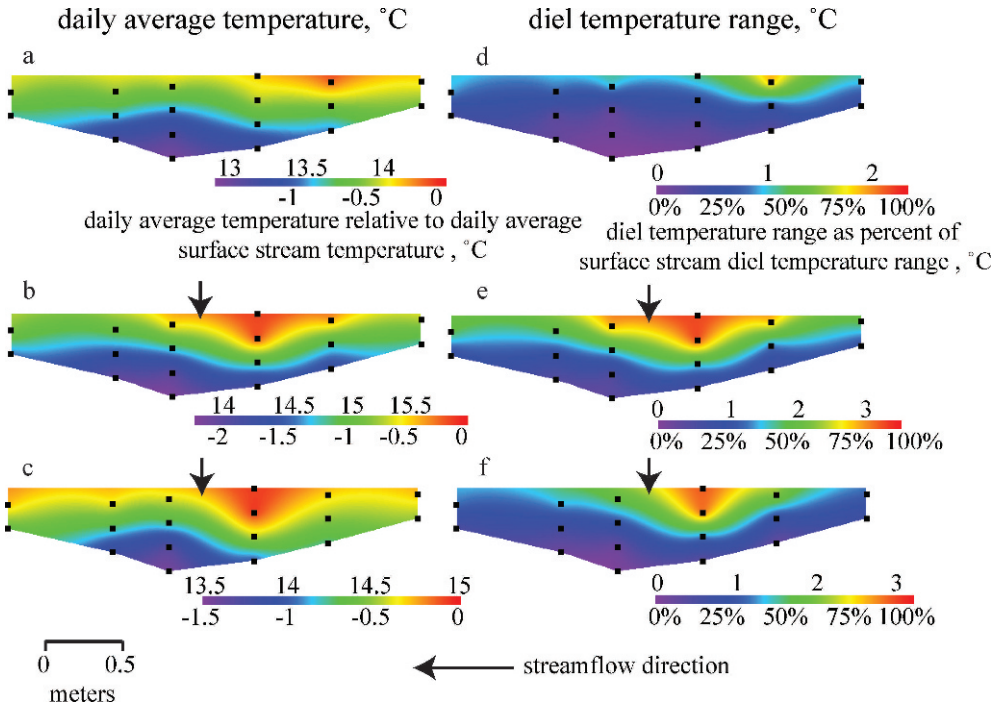

Fig. 5. Longitudinal vertical slices through subsurface water temperature data showing daily average temperature for (a) no weir, (b) 7.6-cm weir, and (c) 15.2-cm weir, and diel temperature range for (d) no weir, (e) 7.6 cm weir, and (f) 15.2 cm weir. Data shown are for representative dates within each weir height experimental period in 2007 (05 June 2007 for panels a and d, 17 June 2007 for panels b and e, and 10 June 2007 for panels c and f). Patterns in 2006 data (not shown) are similar. Arrows show location of weir; filled squares show locations of iButton sensors. Relative temperature scales beneath color bars are relative to daily average temperatures (a, b, c) or diel temperature ranges (d, e, f) for surface stream location marked by circle in Fig. 4a. Data are from left column of iButtons (*see* Methods; Fig. 1) because of its more complete data set. Plots created using Surfer with kriging interpolation using default settings.

through the hyporheic flow cell and thus imparted a cooling effect on the surface stream when the hyporheic water discharged downstream of the weir (Fig. 8a).

The general pattern of weir-induced hyporheic temperature modifications observed at our site is consistent with a large body of literature. Surface water temperatures have been shown to propagate further into subsurface water in areas of downward hyporheic flow or groundwater recharge from surface water than in areas of upward hyporheic flow or groundwater discharge to surface water (Lapham 1989; Stonestrom and Constantz 2003; Anderson 2005). Furthermore, the observed drop in shallow hyporheic temperature downstream across the weir is consistent with other summertime studies that show similar temperature drops across steps (Moore et al. 2005) and riffles (White et al. 1987; Hendricks and White 1991; Evans and Petts 1997). In contrast, such temperature drops are only sometimes observed at gravel bars (Fernald et al. 2006;

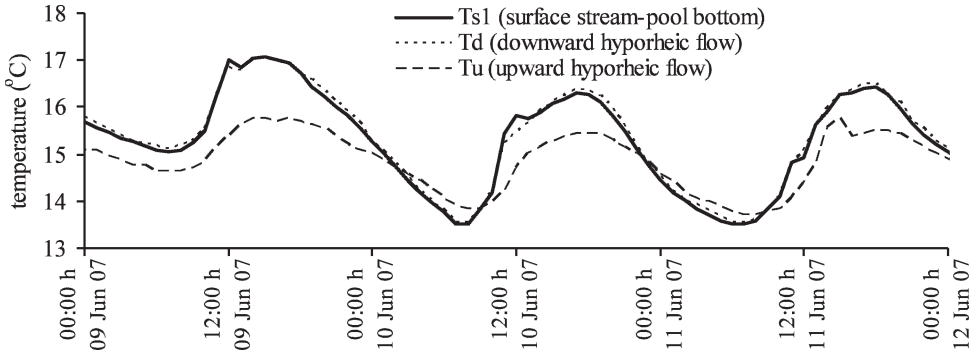

Fig. 6. Example hourly temperatures at beginning (downward hyporheic flow, T_d) and end (upward hyporheic flow, T_u) of weir-induced hyporheic flow cell, and at bottom of pool behind weir (T_{s1}) for the 15.2-cm weir scenario in 2007. Locations are shown in Fig. 1.

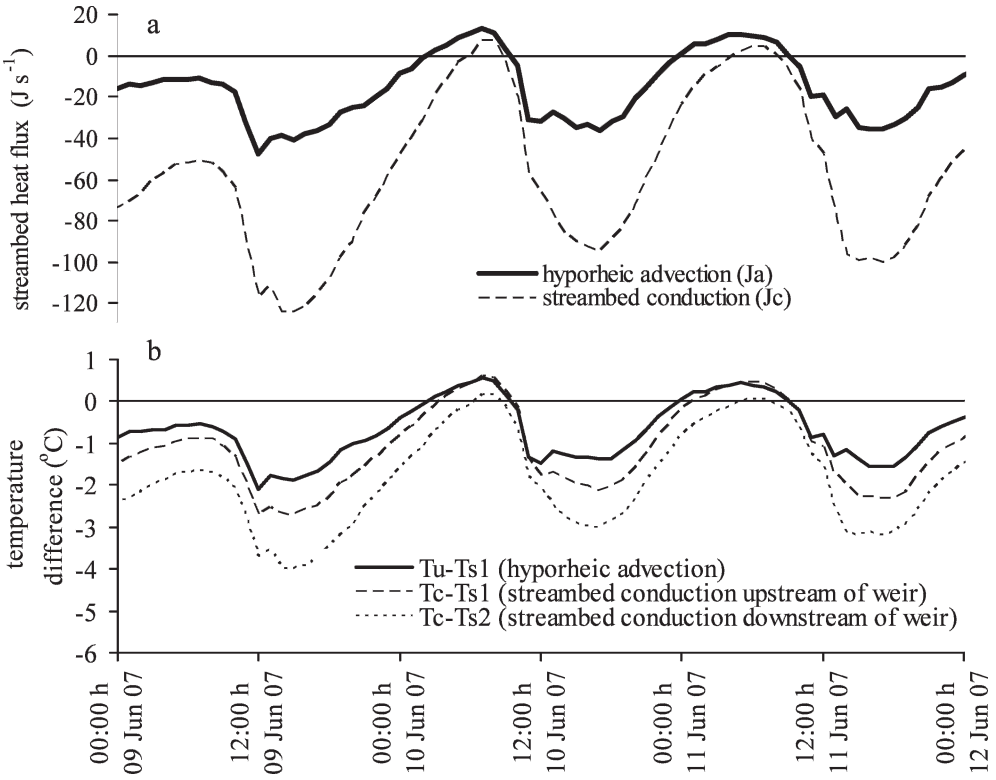

Fig. 7. (a) Example hourly net streambed heat fluxes (net streambed heat conduction, J_c, and net weir-induced hyporheic heat advection, J_a) for the 15.2-cm weir, and (b) example hourly temperature differences used in streambed heat conduction and weir-induced hyporheic heat advection calculations. Net heat fluxes are from perspective of surface stream, so negative values indicate cooling of the surface stream and corresponding warming of the subsurface.

Arrigoni et al. 2008), possibly indicating less interaction of shallow hyporheic flow paths with deeper reservoirs of cooler water or sediments (Fernald et al. 2006).

Observed temperature changes in stream water as it flowed across the weir did not indicate net cooling and were much greater in magnitude than would be expected if either streambed heat conduction (J_c) or weir-induced hyporheic heat advection (J_a) were dominating the surface stream heat budget (Figs. 7–10). Atmospheric heat flux processes (net radiation, sensible heat transfer, evaporation, and condensation) across the stream surface were therefore probably responsible for the majority of observed downstream surface water temperature changes across the weir. Although we did not measure atmospheric heat flux processes, they are probably important because there appears to be significant surface heating in the pool behind the weir (Fig. 4a). This is consistent with studies that have shown atmospheric heat flux processes to dominate the heat budgets of many streams (Brown 1969; Sinokrot and Stefan 1993; Webb and Zhang 2004), sometimes even where heat advection across the streambed is important (Evans et al. 1998; Moore et al. 2005), and particularly where riparian shading had been removed (Johnson 2004).

Weir height was positively correlated with J_a (Fig. 8a), and therefore, with cooling effect on surface water (Fig. 10a), and relative magnitude of J_a to J_c (Fig. 8c). Weir height explained >50% of the variation in J_a. The weir's effect on J_a was due mainly to increased weir-induced hyporheic water exchange (Q_d, Eq. 3; *see* also fig. 9 in Hester and Doyle 2008). Although the magnitude of J_a is directly dependent on the hydraulic conductivity of the sediments (K), the trend of increasing J_a with increasing weir height should be independent of K. Because the stream is hydrologically neutral to gaining, the weir-induced hyporheic flow cell may divert catchment groundwater that would otherwise discharge to the stream at that location. Our experiment does not address this issue, but it seems likely that such diverted catchment groundwater would discharge to the stream elsewhere in the reach, with minimal overall effect to this component of the stream heat budget.

J_c was also generally a cooling influence on the surface stream, and was generally larger than J_a, although still within an order of magnitude (Fig. 8a,b). This is consistent with Peclet numbers near but generally below unity (Fig. 8c). J_c did not exhibit a consistent response to weir height, consistent with an increase in weir height leading to an increase in mixing between the weir-induced hyporheic flow cell and cooler deeper groundwater. In contrast, if the hyporheic flow cell remained largely separate from deeper groundwater, a decrease in J_c with increasing weir height would be expected as the cooler groundwater was pushed further down into the streambed, and vertical thermal gradients consequently declined. Variation in J_c with weir height is therefore most likely caused by variation in

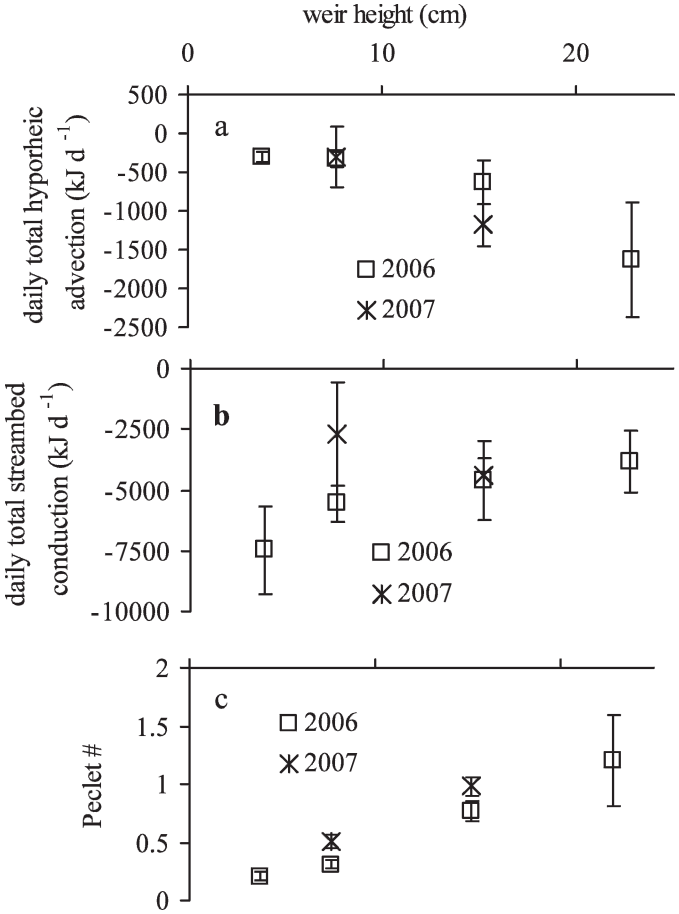

Fig. 8. Daily total streambed heat flux vs. weir height: (a) net weir-induced hyporheic heat advection, J_a, and (b) net streambed heat conduction, J_c. Average Peclet number vs. weir height (c). Boxes and whiskers represent averages and standard deviations, respectively, for entire period that weir was at the given height. Net heat fluxes are from perspective of surface stream, so negative values indicate cooling of the surface stream and corresponding warming of the subsurface. Note difference in y-axis scales between (a) and (b).

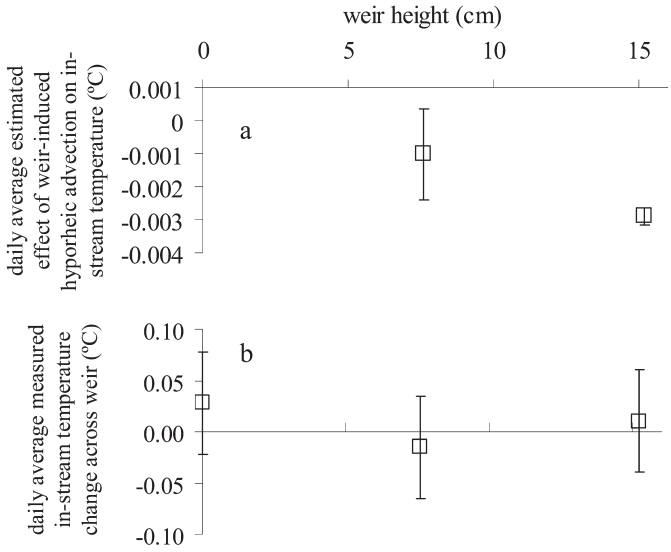

Fig. 10. (a) Daily average estimated effect of net weir-induced hyporheic heat advection on surface stream temperature (daily average ΔT_a, Eq. 7) vs. weir height, and (b) daily average measured temperature change of water upstream to downstream across weir (daily average $Ts_2 - Ts_3$, Fig. 1) vs. weir height for 2007 experiment. Boxes and whiskers represent means and standard deviations, respectively, of the daily averages for entire period that weir was at the given height. Note that negative net heat flux cools the surface stream and warms the subsurface water, and although the magnitude of the ordinate values for both y-axes are less than the accuracy and precision of the iButton sensors, because the values are averages of temperature differences that have at least one significant figure, the rules of significant figures indicate at least one significant figure in the averages.

surface stream temperature because of weather variability. Our results are for a summer experiment; the relative magnitudes of J_a and J_c, as well as the trend of J_a with weir height, may vary with season.

Effect of stream context: Hyporheic heat advection across the streambed induced by an individual weir (J_a)

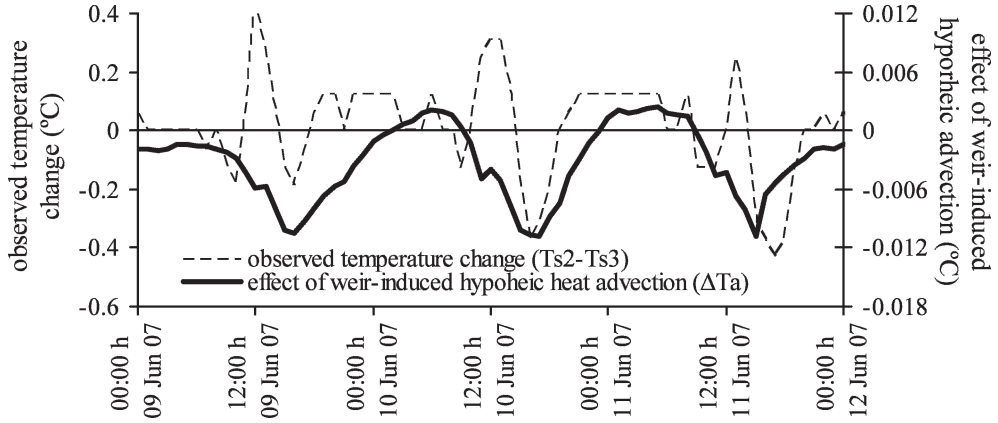

Fig. 9. Example measured temperature change of surface stream water upstream to downstream across weir ($T_{s2} - T_{s3}$, Fig. 1), and estimated effect of net weir-induced hyporheic heat advection on surface stream temperature (ΔT_a). Discretization of measured temperature change is because of resolution of the sensors (0.125°C).

caused local anomalies of subsurface water temperatures (Figs. 4, 5), a response that is expected to be widespread among different streams. However, in contrast with many studies that have linked hyporheic water exchange with surface stream temperature effects (Bilby 1984; Moore et al. 2005; Loheide and Gorelick 2006), our estimates indicate that weir-induced hyporheic heat advection had negligible effect on surface stream temperature (ΔT_a; Figs. 9, 10).

Variation among different streams of ΔT_a induced by a given weir height (and hence the relative magnitudes of J_a and J_c) can be understood by evaluating the relative importance of the various hydrologic and geomorphic contextual parameters represented by each of the input variables in Eq. 7. We discuss these parameters in descending order of importance. The most important parameter in controlling ΔT_a is sediment hydraulic conductivity (K, a function of sediment texture), which varies directly with ΔT_a, and can vary among streams by nearly 10 orders of magnitude, ranging from bedrock to very coarse alluvium (Freeze and Cherry 1979; Calver 2001). For J_a to dominate relative to J_c, and for ΔT_a to be ecologically relevant, it appears that K would need to be at least an order of magnitude greater than estimated for our experimental site (i.e., $>\sim 10^{-3}$ m s^{-1}, corresponding to fine gravel). In most settings, the second most important parameter is surface stream discharge (Q_s), which varies inversely with ΔT_a, and can vary over at least four orders of magnitude between streams (Leopold and Maddock 1953), but can also vary widely among seasons and weather conditions in a given stream. Temperature differences between the surface stream and the weir-induced hyporheic flow cell ($T_u - T_{s3}$) and hydraulic gradients induced by a given weir (i_d) both vary directly with ΔT_a and should vary less than an order of magnitude between streams, but also vary over time and with structure height in a given stream. Temperature differences may also vary between different structure types and shady vs. sunny reaches. The area of downward hyporheic flow across the streambed (A_d) also varies directly with ΔT_a over a couple orders of magnitudes between streams. Much of this variation is attributable to channel width, although some may also be attributable to structure height.

Although streambed heat conduction (J_c) does not vary directly with K (Eq. 5), an increase in K would increase Q_d, which might decrease the temperature difference between the surface stream and subsurface water upstream of the weir ($T_c - T_{s1}$) and increase the temperature difference downstream of the weir ($T_c - T_{s2}$). Because J_c is a summation of conduction upstream and downstream of the weir, the effect of K on thermal gradients in these two areas may partially cancel out, with little net effect on J_c. This is an area for future research. Independent of variation in K, $T_c - T_{s1,2}$ and the area of the streambed of interest (A_c, in terms of channel width) are the only parameters in Eq. 5 that vary considerably between streams, and such variations influence J_a in much the same way they influence J_c. For this reason, sediment texture, through its wide natural variability and control of K, is the primary control on the relative magnitudes of J_a and J_c (Cardenas and Wilson 2007). Therefore, although J_a and J_c happen to be of a similar order of magnitude in our study (Fig. 7a), their relative magnitude could vary markedly between sites.

Parameter uncertainty: The degree of uncertainty associated with each of the input parameters in Eqs. 1–7 varies widely among the parameters, and this has important implications for the conclusions presented in this paper. Sediment hydraulic conductivity (K) is highly heterogeneous in streambeds (Cardenas and Zlotnik 2003) and the falling-head tests used in this study measure K only in relatively small areas in the vicinity of the test piezometer. Further, K can vary over many orders of magnitude (Freeze and Cherry 1979; Calver 2001), and is therefore by far the most uncertain parameter in our calculations, and the only one that can affect our conclusions that rest on the magnitude of weir-induced hyporheic heat advection (J_a; Figs. 7a, 9). Uncertainty in our estimate of weir-induced hyporheic heat advection is equal to the uncertainty associated with each factor in Eq. 3. For example, if our estimate of K were off by a factor of 10, the weir-induced hyporheic heat advection calculation would be off by the same factor. A minimum level of uncertainty in K can be estimated as the ratio of largest to smallest measured K values from falling-head tests (1.03 in 2006 and 5.92 in 2007). Regardless of the direction of the error, an order-of-magnitude error in K would invalidate the conclusion that streambed heat conduction (J_c) and J_a are of similar magnitude (Fig. 7a). Further, the conclusion that weir-induced hyporheic advective effects on surface stream temperature (ΔT_a) are negligible (Fig. 9) would be invalidated if K was underestimated by an order of magnitude. ΔT_a would increase by a factor of 10 to peak at approximately 0.1°C rather than 0.01°C (Fig. 9), which has potential to be important both in terms of the surface stream heat budget and ecologically.

In contrast, all other sources of uncertainty in Eqs. 1–7 (e.g., those associated with methods for estimating upwelling area (A_u) from downwelling area (A_d), choice of piezometer locations used to represent hydraulic gradient or temperature, and methods for measuring surface stream discharge) are far smaller than that for K (i.e., less than an order of magnitude) and consequently would not affect those conclusions that rest on the order of magnitude of weir-induced hyporheic heat advection. Finally, none of the input parameter uncertainty has the potential to affect our remaining conclusions, which are based on temperature or hydraulic head patterns (Figs. 2–6, 7b, 10b) or trends of response to weir height (Figs. 8, 10a).

Ecological significance: The effects of in-stream geomorphic structures on stream temperature presented in this paper help us understand one way in which these common structures may affect ecological stream function in summer. For instance, thermal heterogeneity induced in the surface stream and shallow hyporheic zone (and therefore benthic zone) and by our experimental structure (~1.0°C; Figs. 4, 5), may be large enough to have direct ecological consequences. On the other hand, the thermal effect of hyporheic heat advection induced by our single experimental structure on bulk summer surface stream temperatures (<0.01°C; Fig. 9),

as estimated in this study, would be negligible. These conclusions may vary among streams and seasons, particularly the hyporheic effect on surface stream temperatures, which could vary widely with sediment hydraulic conductivity. Furthermore, we did not address the cumulative hyporheic effect of multiple structures, which may be greater.

Organisms are adapted to the thermal regimes typically experienced in their native ranges (Hill et al. 2004; Lomolino et al. 2006), and are therefore sensitive to human-induced thermal shifts (Walther et al. 2002). Mechanisms of human effects on stream temperature include loss of riparian shading, reduction of groundwater input and hyporheic exchange, and global warming (Pilgrim et al. 1998; Poole and Berman 2001). Thermal effects of structure-induced hyporheic exchange may therefore prove beneficial in helping mitigate human-induced thermal stress in streams. For example, enhanced thermal heterogeneity induced by structures may provide thermal refugia for organisms inhabiting the hyporheic zone, the benthic zone, or the water column. Furthermore, in settings where structure-induced hyporheic exchange has significant effect on surface stream temperatures (e.g., coarse streambeds), moderation of daily or annual peak temperatures may help buffer stream temperatures against human activities. Finally, although our focus has been temperature, structures can have other ecologically relevant functions, such as trapping woody debris, grade control, habitat creation, and other hyporheic functions (e.g., nutrient processing) (Doll et al. 2003; Lautz and Fanelli in press).

References

Anderson, M. P. 2005. Heat as a ground water tracer. Ground Water **43:** 951–968.

Arrigoni, A. S., G. C. Poole, L. A. K. Mertes, S. J. O'Daniel, W. W. Woessner, and S. A. Thomas. 2008. Buffered, lagged, or cooled? Disentangling hyporheic influences on temperature cycles in stream channels. Water Resour. Res **44:** W09418, doi: 10.1029/2007WR006480.

Begon, M., C. R. Townsend, and J. L. Harper. 2006. Ecology, 4th ed. Blackwell.

Bilby, R. E. 1984. Characteristics and frequency of cool-water areas in a western Washington stream. J. Freshw. Ecol. **2:** 593–602.

Brown, G. W. 1969. Predicting temperatures of small streams. Water Resour. Res. **5:** 68–75.

Brown, J. H., J. F. Gillooly, A. P. Allen, V. M. Savage, and G. B. West. 2004. Toward a metabolic theory of ecology. Ecology **85:** 1771–1789.

Brunke, M., and T. Gonser. 1997. The ecological significance of exchange processes between rivers and groundwater. Freshw. Biol. **37:** 1–33.

Calver, A. 2001. Riverbed permeabilities: Information from pooled data. Ground Water **39:** 546–553.

Cardenas, M. B., and J. L. Wilson. 2007. Effects of current-bed form induced fluid flow on the thermal regime of sediments. Water Resour. Res. **43:** W08431, doi: 10.1029/2006WR005343.

———, and V. A. Zlotnik. 2003. Three-dimensional model of modern channel bend deposits. Water Resour. Res. **39:** 1141, doi: 10.1029/2002WR001383.

Crisp, D. T. 1990. Water temperature in a stream gravel bed and implications for salmonid incubation. Freshw. Biol. **23:** 601–612.

Doll, B. A., G. L. Grabow, K. R. Hall, J. Halley, W. A. Harman, G. D. Jennings, and D. E. Wise. 2003. Stream restoration: A natural channel design handbook. NC Stream Restoration Institute, NC State Univ.

Evans, E. C., G. R. McGregor, and G. E. Petts. 1998. River energy budgets with special reference to river bed processes. Hydrol. Processes **12:** 575–595.

———, and G. E. Petts. 1997. Hyporheic temperature patterns within riffles. Hydrol. Sci. J./J. Sci. Hydrol. **42:** 199–213.

Fernald, A. G., D. H. Landers, and P. J. Wigington. 2006. Water quality changes in hyporheic flow paths between a large gravel bed river and off-channel alcoves in Oregon, USA. River Res. Appl. **22:** 1111–1124.

Freeze, R. A., and J. A. Cherry. 1979. Groundwater. Prentice-Hall.

Gooseff, M. N., J. K. Anderson, S. Wondzell, J. Lanier, and R. Haggerty. 2006. A modeling study of hyporheic exchange pattern and the sequence, size, and spacing of stream bedforms in mountain stream networks, Oregon, USA [retraction of **19**: 2915–2929, 2005]. Hydrol. Processes **20:** 2443–2457, doi: 10.1002/hyp.6349.

Hansen, E. A. 1975. Some effects of groundwater on brown trout redds. Trans. Am. Fish. Soc. **104:** 100–110.

Hendricks, S. P., and D. S. White. 1991. Physicochemical patterns within a hyporheic zone of a northern Michigan river, with comments on surface-water patterns. Can. J. Fish. Aquat. Sci. **48:** 1645–1654.

Hester, E. T., and M. W. Doyle. 2008. In-stream geomorphic structures as drivers of hyporheic exchange. Water Resour. Res. **44:** W03417, doi: 10.1029/2006WR005810.

Hill, R. W., G. A. Wyse, and M. Anderson. 2004. Animal physiology. Sinauer.

Hondzo, M., and H. G. Stefan. 1994. Riverbed heat-conduction prediction. Water Resour. Res. **30:** 1503–1513.

Hynes, H. B. N. 1970. The ecology of running waters. Univ. of Toronto Press.

Jobson, H. E. 1977. Bed conduction computation for thermal models. J. Hydraul. Div. Proc. Am. Soc. Civ. Eng. **103:** 1213–1217.

Johnson, A. N., B. R. Boer, W. W. Woessner, J. A. Stanford, G. C. Poole, S. A. Thomas, and S. J. O'Daniel. 2005. Evaluation of an inexpensive small-diameter temperature logger for documenting ground water-river interactions. Ground Water Monit. Remediat. **25:** 68–74.

Johnson, S. L. 2004. Factors influencing stream temperatures in small streams: Substrate effects and a shading experiment. Can. J. Fish. Aquat. Sci. **61:** 913–923.

Jones, J. B., and P. J. Mulholland. 2000. Streams and ground waters. Academic Press.

Kasahara, T., and S. M. Wondzell. 2003. Geomorphic controls on hyporheic exchange flow in mountain streams. Water Resour. Res. **39:** 1005, doi: 10.1029/2002WR001386.

Lapham, W. W. 1989. Use of temperature profiles beneath streams to determine rates of vertical ground-water flow and vertical hydraulic conductivity. U.S. Geological Survey Water-Supply Paper 2337.

Lautz, L., and R. Fanelli. In press. Seasonal biogeochemical hotspots in the streambed around restoration structures. Biogeochemistry.

Leopold, L. B., and T. J. Maddock. 1953. The hydraulic geometry of stream channels and some physiographic implications. U.S. Geological Survey Professional Paper 252.

Lindeburg, M. R. 2001. Civil engineering reference manual, 8th ed. Professional Publications.

Loheide, S. P., and S. M. Gorelick. 2006. Quantifying stream-aquifer interactions through the analysis of remotely sensed thermographic profiles and in situ temperature histories. Environ. Sci. Technol. **40:** 3336–3341.

Lomolino, M. V., B. R. Riddle, and J. H. Brown. 2006. Biogeography, 3rd ed. Sinauer.

Moore, R. D. 2005. Slug injection using salt solution. Streamline Watershed Manage. Bull. **8:** 1–6.

———, P. Sutherland, T. Gomi, and A. Dhakal. 2005. Thermal regime of a headwater stream within a clear-cut, coastal British Columbia, Canada. Hydrol. Processes **19:** 2591–2608.

Pilgrim, J. M., X. Fang, and H. G. Stefan. 1998. Stream temperature correlations with air temperatures in Minnesota: Implications for climate warming. J. Am. Water Resour. Assoc. **34:** 1109–1121.

Poole, G. C., and C. H. Berman. 2001. An ecological perspective on in-stream temperature: Natural heat dynamics and mechanisms of human-caused thermal degradation. Environ. Manage. **27:** 787–802.

———, and others. 2008. Hydrologic spiraling: the role of multiple interactive flow paths in stream ecosystems. River Res. Applic. **24:** 1018–1031, doi: 10.1002/rra.1099.

Ringler, N. H., and J. D. Hall. 1975. Effects of logging on water temperature and dissolved-oxygen in spawning beds. Trans. Am. Fish. Soc. **104:** 111–121.

Silliman, S. E., and D. F. Booth. 1993. Analysis of time-series measurements of sediment temperature for identification of gaining vs losing portions of Juday-Creek, Indiana. J. Hydrol. **146:** 131–148.

Sinokrot, B. A., and H. G. Stefan. 1993. Stream temperature dynamics—measurements and modeling. Water Resour. Res. **29:** 2299–2312.

Stonestrom, D. A., and J. Constantz. 2003. Heat as a tool for studying the movement of ground water near streams. Circular 1260. U.S. Geological Survey.

Story, A., R. D. Moore, and J. S. Macdonald. 2003. Stream temperatures in two shaded reaches below cutblocks and logging roads: Downstream cooling linked to subsurface hydrology. Can. J. For. Res./Rev. Can. Rech. For. **33:** 1383–1396.

Thibodeaux, L. J., and J. D. Boyle. 1987. Bedform-generated convective-transport in bottom sediment. Nature **325:** 341–343.

Vaux, W. G. 1962. Interchange of stream and intragravel water in a salmon spawning riffle.Special Scientific Report—Fisheries No. 405. United States Fish and Wildlife Service.

Walther, G. R., and others. 2002. Ecological responses to recent climate change. Nature **416:** 389–395.

Webb, B. W., and Y. Zhang. 2004. Intra-annual variability in the non-advective heat energy budget of Devon streams and rivers. Hydrol. Processes **18:** 2117–2146.

White, D. S., C. H. Elzinga, and S. P. Hendricks. 1987. Temperature patterns within the hyporheic zone of a northern Michigan river. J. N. Am. Benthol. Soc. **6:** 85–91.

Edited by: Josef D. Ackerman

Received: 06 December 2007
Accepted: 12 September 2008
Amended: 15 September 2008